CHAPTER 4

MECHANICAL PROPERTIES, CORROSION BEHAVIOR AND BIOCOMPATIBILITY OF INDIGENOUSLY DEVELOPED NICKEL-FREE AUSTENITIC STAINLESS STEEL (HNS-Mo)

4.1. Introduction

As shown in the previous chapter, HNS stainless steel exhibits lower pitting potential and also lower high cycle fatigue endurance limit at 10^7 cycles in respect of the 316L. However, there is a chance of pitting corrosion in the 316L and it may release nickel ions during long-term implantation in the human body. Nickel ions cause allergic reactions. In metal allergy, a chemical substance that the human body originally does not have, is generated and biological cells cause rejection reaction against the generated chemical substance; thereby, an abnormality is caused in the human body. To avoid such problems, a new grade of nickel free stainless steel was designed for biomedical applications.

Manganese and molybdenum increase solubility of nitrogen in austenitic stainless steel. However, as mentioned in the previous chapter, Mn has a negative effect on corrosion resistance of the HNS. A very high amount of nitrogen content in stainless steel causes brittleness. High nitrogen-containing stainless steels exhibit ductile to brittle transition temperature (DBTT) [81]. It strongly depends on the nitrogen content and can be predicted according to **Eq. 1.3** [52]. Therefore, there is a limit to the maximum nitrogen content in stainless steel. Also, production of stainless steel with very high nitrogen content (>8000 ppm) is a difficult task for commercial steel plants.

Ahila et al. [88] observed the beneficial effect of nitrogen on repassivation of Cr-Mn steel with both Cr and Mn content of about 19 %. The stainless steel having ~ 0.60 % of nitrogen exhibited an improved repassivation tendency. However, further increase in the

nitrogen content to ~ 0.90 %, did not have significant effect on repassivation behavior of this steel. Therefore, the amount of nitrogen may be limited to 0.60-0.70 % in stainless steels for optimum repassivation and toughness. Pitting resistance of stainless steel is improved by addition of Molybdenum (Mo). Mo as an alloying element in stainless steel reduces both, the number as well as the size of nucleation of metastable pits; but high Mo content in the steel promotes ferrite formation during processing. Also, there is a synergistic effect of nitrogen and molybdenum on the corrosion resistance of stainless steel [64,182]. Therefore, amount of Mo is kept within the restricted limit.

Based on extensive literature review, an attempt was made to develop a medical-grade of austenitic stainless steel, comprising carbon up to 0.05 wt%; manganese in the range of 19-20 wt%; chromium in the range of 19-20 wt%; molybdenum in the range of 0.50-1.0 wt%; nitrogen in the range of 0.60-0.70 wt%; nickel up to 0.10 wt%; silicon up to 0.50 wt%; copper up to 0.10 wt% and balance iron. This investigation aimed to indigenously develop a composition of austenitic stainless steel, free from nickel or with negligible nickel, and characterize its mechanical properties, corrosion behavior and biocompatibility for biomedical applications.

4.2. Microstructure Characterization of HNS-Mo

The optical microstructure of the HNS-Mo is shown in **Fig. 4.1a**. It consists of equiaxed austenite grains with few annealing twins without significant ferrite phase. The ASTM grain size number was found to be 6 and that is in accordance with the ISO 5832-1 standard. Carbide precipitation was not observed at grain boundaries. X-ray diffraction pattern (with Cu-Kα radiation) of the HNS-Mo is shown in **Fig. 4.1b**. Only the peaks of austenite may be observed. The inclusion rating of this steel is given in **Table 4.1**. It is found within the limit, as per the ISO 5832-1 standard.

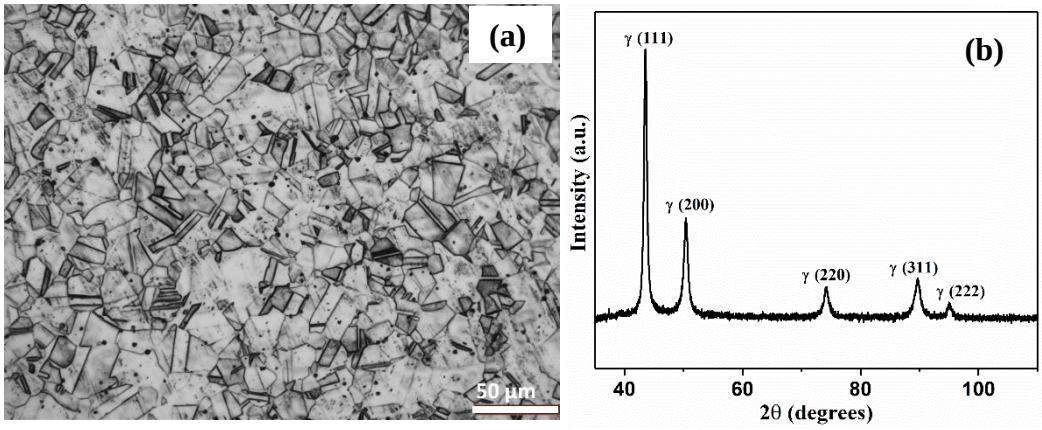

Fig. 4.1. (a) Optical micrograph, and (b) X-ray diffraction pattern of the HNS-Mo austenitic stainless steel.

Table 4.1. Inclusion rating of the HNS-Mo austenitic stainless steel.

Types of inclusion	**A**		**B**		**C**		**D**	
	Thin	**Heavy**	**Thin**	**Heavy**	**Thin**	**Heavy**	**Thin**	**Heavy**
Determined values	1	1	1	Nil	Nil	Nil	1.5	0.5
Permissible limit (ISO 5832-1)	1.5	1	1.5	1	1.5	1	1.5	1

4.3. Corrosion Behavior of HNS-Mo

Corrosion tests were performed to evaluate pitting and intergranular corrosion resistance of the HNS-Mo. A step-like structure was observed on etching with 10 % oxalic acid according to the ASTM A-262 practice A **(Fig. 4.2)**.

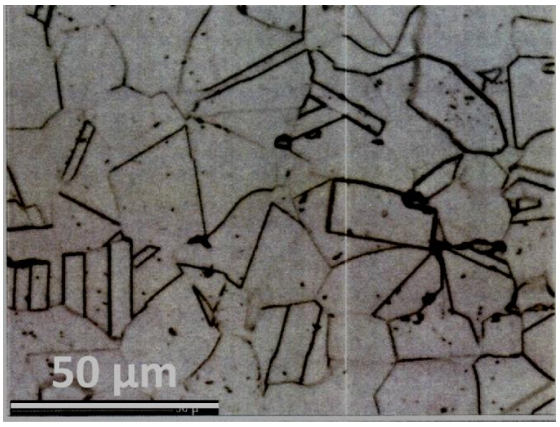

Fig. 4.2. Microstructure of the HNS-Mo austenitic stainless steel, following 10% oxalic acid test according to ASTM A-262, practice A.

Fissures were absent after 15 h of boiling in copper-copper sulphate, 16% sulphuric acid solution. The microstructure was found free from intergranular corrosion and grain dropping, according to ASTM A-262 practice E. Corrosion rate of 15.26 g/m^2 was observed in 6% $FeCl_3$ solution for the HNS-Mo, according to the ASTM G 48-11 Method-A. This value was found 48.52 g/m^2 and 368.88 g/m^2 for the HNS and 316L, respectively. The maximum depth of attack was found to be 0.09 mm for the HNS-Mo at 22ºC for 24 h of exposure, on testing according to ASTM G 48-11 Method-D.

Electrochemical corrosion resistance was studied using potentiodynamic polarization. **Fig 4.3** shows the potentiodynamic polarization behavior of the HNS-Mo along with those of the HNS and 316L. The various corrosion data were estimated from the potentiodynamic curves and these are presented in **Table 4.2**. It may be seen from **Fig. 4.3** that HNS-Mo has higher breakdown potential than HNS and it is equivalent to that of the 316L **(Table 4.2)**. The corrosion potential of the HNS-Mo is similar to that of the 316L. However, the critical current density of the HNS-Mo is lower than that of the 316L, which signifies the better corrosion resistance of the HNS-Mo in Ringer's solution compared to that of the 316L.

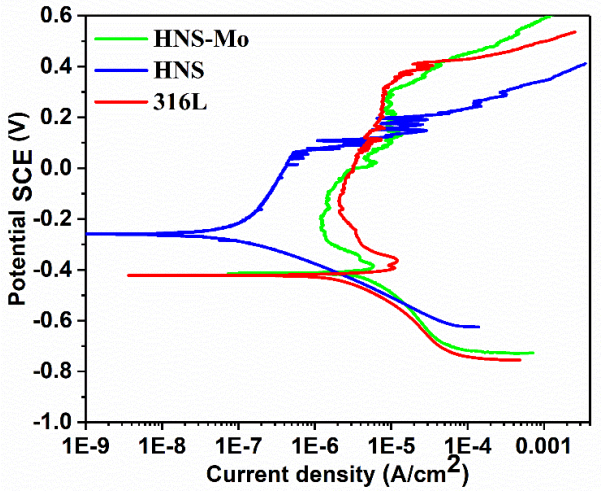

Fig. 4.3. Potentiodynamic polarization curves of the HNS-Mo, HNS and 316L austenitic stainless steels.

Table 4.2. Corrosion data of the HNS-Mo, HNS and 316L austenitic stainless steels.

Material	Corrosion potential, E_{corr} (mV_{SCE})	Breakdown potential (mV)	Critical current density, i_{cr} ($\mu A/cm^2$)	Current density i_{corr} at 200 mV ($\mu A/cm^2$)
316L	-421	316	11.8	7.45
HNS	-260	196	0.11	27.5
HNS-Mo	-413	310	5.78	10.3

4.4. Comparison of Mechanical Properties of the HNS-Mo, HNS and 316L

Various mechanical properties of the HNS-Mo were determined by tensile test, stress-controlled high cycle fatigue test and corrosion fatigue test. Load-bearing implants are exposed to cyclic loading during service and may fail due to the combined effect of corrosion and fatigue. Therefore, high cycle fatigue and corrosion fatigue of the HNS-Mo were studied and compared with those of the HNS and 316L.

4.4.1. Tensile Properties and Hardness

The engineering stress-strain plot of the HNS-Mo is compared with those of the HNS and 316L, as shown in **Fig. 4.4.**

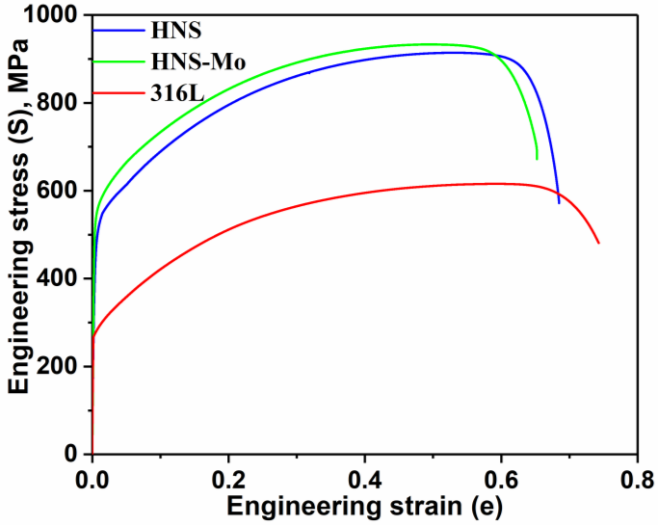

Fig. 4.4. Comparison of engineering stress-strain curves of the HNS-Mo, HNS and 316L austenitic stainless steels.

The various parameters were evaluated and are presented in **Table 4.3**. It may be observed that the HNS-Mo shows the highest yield strength and tensile strength, whereas its ductility is lower compared to those of the HNS and 316L. However, it is having a sufficiently high uniform strain of 50%. The Vickers hardness of the HNS-Mo was found 286 ± 4 Hv, which is about two times that of the 316L (140 ± 6 Hv).

Table 4.3. Tensile properties of the HNS-Mo, HNS and 316L austenitic stainless steels.

Material	Yield strength (MPa)	Ultimate tensile strength (MPa)	Uniform strain (%)	Total strain (%)	UTS/YS
316L	279	616	58	74	2.21
HNS	525	914	52	68	1.74
HNS-Mo	540	933	50	65	1.73

4.4.2. High Cycle Fatigue Behavior of the HNS-Mo in Air

The high cycle fatigue behavior of the HNS-Mo was studied and is compared with those of the HNS and 316L. **Fig. 4.5a** shows the stress-number of cycles (S-N) curves of all the three austenitic stainless steels, tested in air at a stress ratio (R) of 0.1.

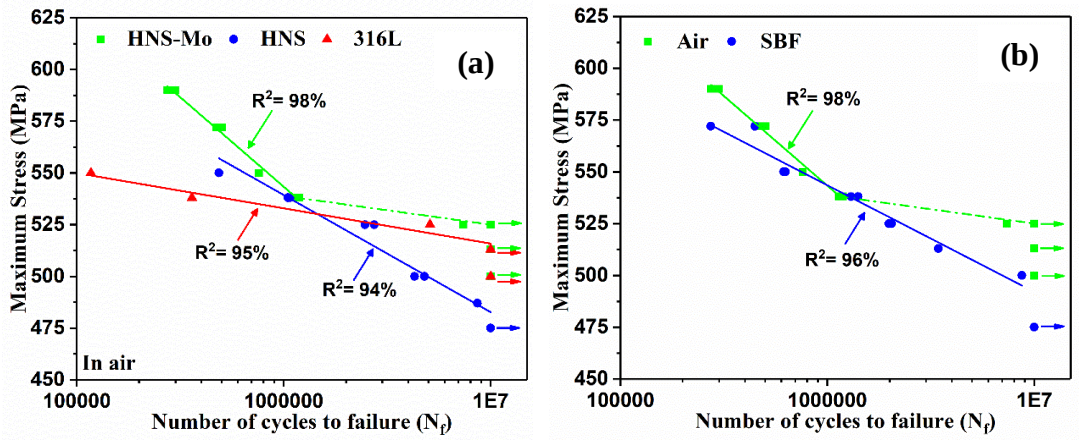

Fig. 4.5. (a) Comparison of high cycle fatigue behavior of the HNS-Mo, HNS and 316L austenitic stainless steels in the air, and (b) Comparison of high cycle fatigue behavior of the HNS-Mo in air and SBF, at stress ratio of 0.1.

The fatigue life of the HNS-Mo is highest, irrespective of the stress amplitude, as shown in **Table 4.4**. The number of cycles to failure was found to increase with decreasing stress for all the three steels. The maximum stress corresponding to the endurance limit of HNS-Mo at 10^7 cycles is 513 MPa.

Table: 4.4. Comparison of high cycle fatigue life of the HNS-Mo, HNS and 316L austenitic stainless steels at various maximum stresses.

Maximum stress, MPa	**Fatigue life (N_f)**			
	HNS	**316L**	**HNS-Mo (air)**	**HNS-Mo (SBF)**
590	-	-	298377	
			274646	
572	-	-	505170	273673
			471045	447361
550	486013	117046	759624	615223
				628543
538	1049450	360417	1136100	1303120
	1073080		1188830	1408250
525	2739134	5093733	7389220	1984250
	2470231		NF	2045300
513		NF	NF	3443620
500	4797074	NF	NF	8721000
	4292637			
475	NF	-	-	NF

Note: NF: not failed for 10^7 cycles

4.4.3. Corrosion Fatigue of HNS-Mo

The human body fluid environment is highly corrosive. The effect of SBF environment (Ringer's solution) on the stress-controlled fatigue behavior was studied. The fatigue life data related to various maximum stresses are presented in **Table 4.4**. The S-N curves for the HNS-Mo in air and SBF are shown in **Fig. 4.5b**. SBF has a significant effect on the

fatigue life at lower stress levels, whereas a little effect was observed at the higher stress level. The endurance limit was reduced to 475 MPa in SBF from 513 MPa in air.

4.5. Biocompatibility of HNS-Mo

4.5.1. *In vitro* Cell Adhesion and Proliferation

Figs. 4.6 shows the adhesion of L-929 cells on the HNS-Mo austenitic stainless steel. L-929 cells are well adhered and spread on the HNS-Mo and control glass coverslip. The coverage of MG-63 cells increased gradually for all the three steels with the duration of incubation, as shown in **Fig. 4.7**. Cell proliferation of MG-63 cells on the three steels was evaluated using the MTT assay method, as described in **chapter 2**. There is a gradual increase in the mean percentage of cell proliferation for the three materials with the duration of incubation, as shown in **Fig. 4.8**. It can be seen that there is a significant difference at the level of 0.05 between different time points for the MG-63 cells for all the samples. However, there is a significant increase in cell proliferation for the HNS-Mo compared to 316L and HNS after 3 days of incubation.

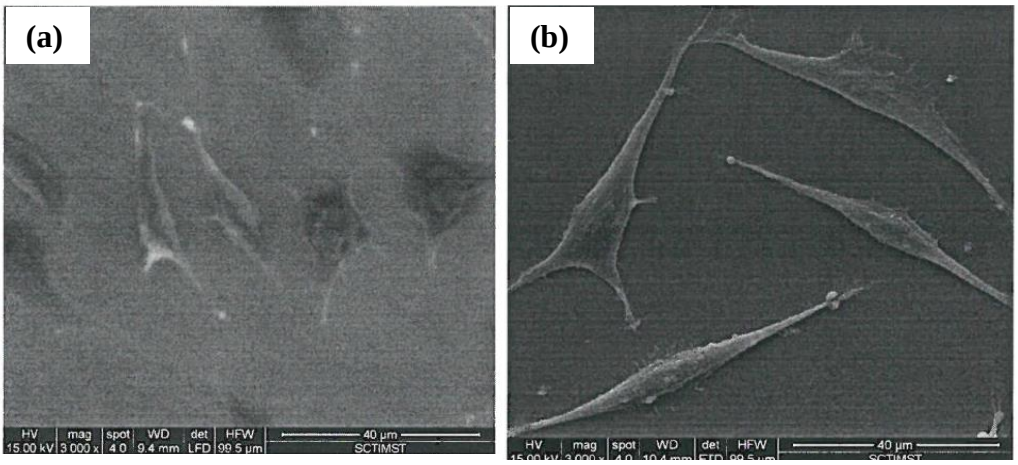

Fig. 4.6. L-929 cells adhesion on (a) HNS-Mo and (b) glass coverslip.

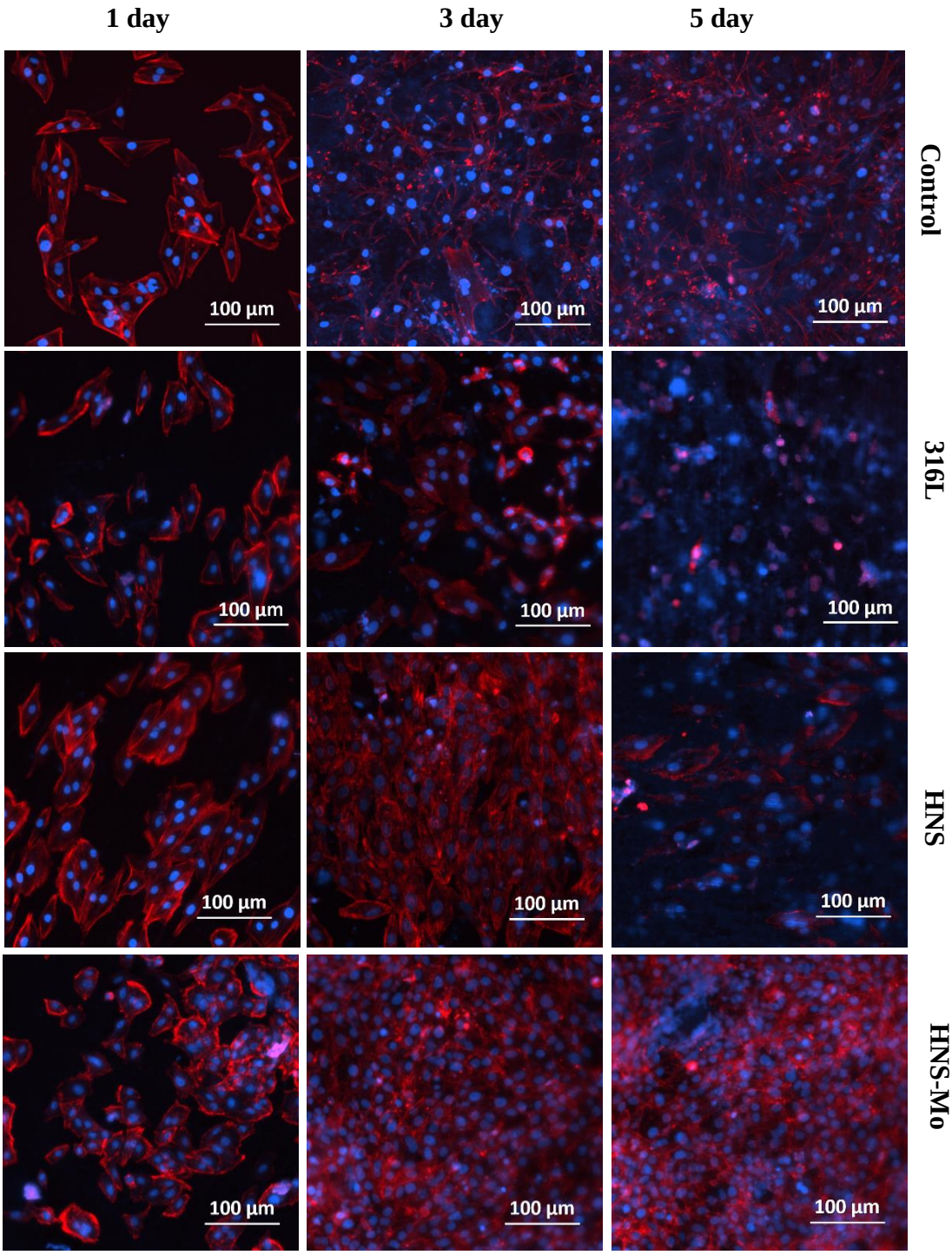

Fig. 4.7. Panel representing the fluorescent cell culture images of the MG-63 human bone osteosarcoma cells on the various steel samples; after 1 day, 3 days and 5 days of incubation. Blue color: nuclei staining; red color: actin cytoskeleton filament staining.

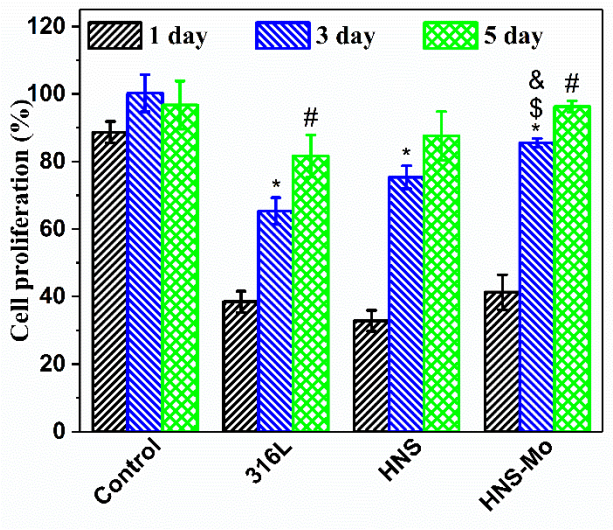

Fig. 4.8. Histograms representing comparison of the MG-63 cell proliferation on the 316L, HNS and HNS-Mo austenitic stainless steels after 1, 3 and 5 days of incubation by MTT assay. In this experiment, the absorbance of control for the 5th-day culture was taken as a reference for all the samples. $^{*}p \leq 0.05$ with respect to 1 day of the corresponding group. $^{\#}p \leq 0.05$ with respect to 3 days of the corresponding group. $^{\$}p \leq 0.05$ with respect to 316L for the same day. $^{\&}p \leq 0.05$ with respect to HNS for the same day.

4.5.2. *In vitro* Cytotoxicity

The cytotoxicity reactivities of HNS-Mo and control samples were evaluated under an inverted phase-contrast microscope based on various grading (**Fig. 4.9**) and the results are presented in **Table 4.5**. As per the ISO 10993-5, achieving a numerical grade of more than two is considered a cytotoxic effect. HNS-Mo achieved a numerical grade of 0. Negative control exhibited none cytotoxic reactivity and positive control showed severe cytotoxic reactivity as expected.

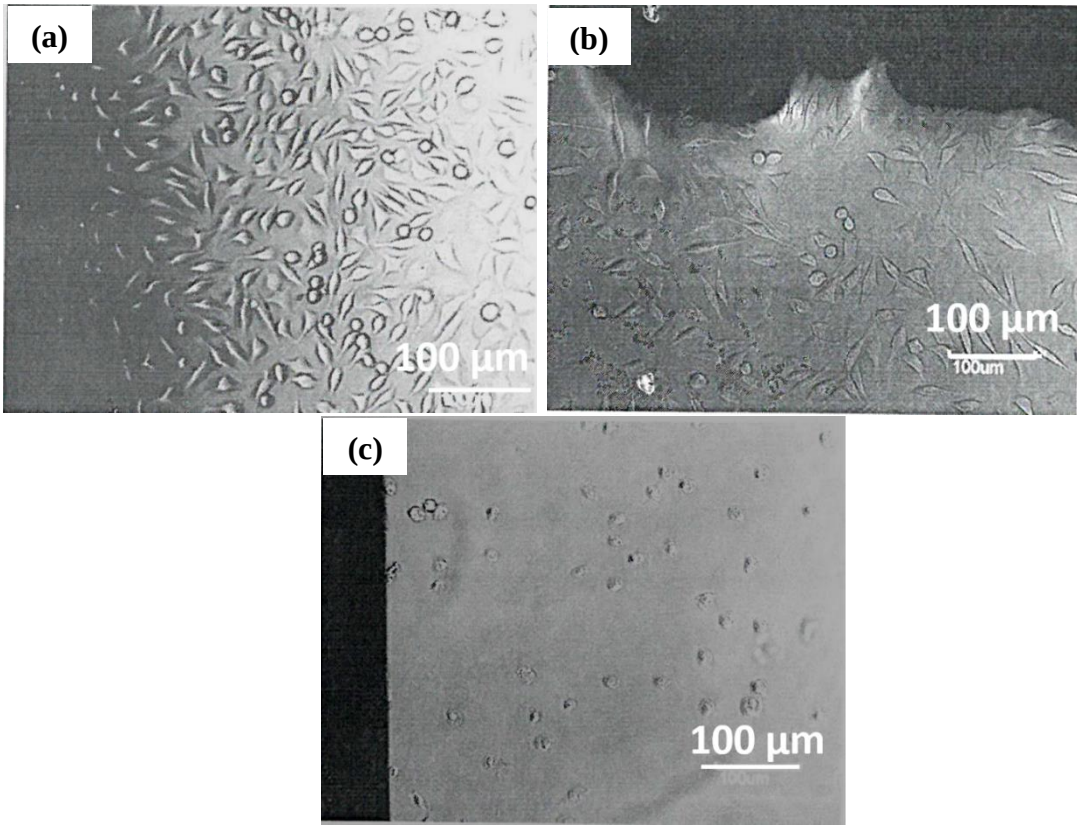

Fig. 4.9. L-929 cells after 24 h contact with (a) HNS-Mo austenitic stainless steel, (b) negative control (UHMWPE) and (c) positive control (PVC).

Table 4.5. Grading of reactivity of cells.

Sample	Grade	Reactivity
Negative control	0	None
Positive control	4	Severe
HNS-Mo	0	None

4.5.3. Hematology

The percent hemolysis in plasma samples, after exposure to the HNS-Mo, was found within the normal hemolysis (< 0.10%). The percent change in leukocyte count in blood for the HNS-Mo was found 1.28, whereas it was 3.34 ± 0.46 (n=3) in references after 30 min of exposure, where the uncertainty in measurement was ± 5%. The change in platelet count detected in blood for HNS-Mo was found 9.95%, 10.73% and 6.73, whereas, in

references, it was 6.41 ± 2.40 (n=3) after 30 min of exposure, where the uncertainty of measurement was ± 10%.

4.5.4. *In vivo* Studies

Various *in vivo* studies were conducted according to the ISO standard to evaluate the biocompatibility of the HNS-Mo austenitic stainless steel. The results are as follows:

4.5.4.1. Irritation and Skin Sensitization

The PS and CSO extracts of the HNS-Mo induced a total mean score of "0" in PS extracts and "0.33" in CSO extracts, following intradermal injections. Hence, the PS and CSO extract of the HNS-Mo meet the test requirements as per ISO 10993-10: 2010 (E): Biological evaluation of medical devices: Part 10: Tests for irritation and skin sensitization: Clause 6.4: Animal Intracutaneous (Intradermal) reactivity test. Animals did not show any abnormality throughout the experiment after intradermal injection. There was no mortality.

The results of the GPMT test were evaluated on the basis of the skin sensitization (erythema and oedema) potential induced by the test material (HNS-Mo), indicating that the PS extract of the HNS-Mo and control-treated animals did not show any adverse skin reaction during the induction of challenge period and confirmed that the PS extract of the test material is a non-irritant in laboratory condition. Hence, the PS extracts of the HNS-Mo meet the requirement of the test as per the ISO 10993-10: 2010 (E): Biological evaluation of medical devices: Part 10: Tests for irritation and skin sensitization: Clause 7.5: Guinea pig maximization test (GPMT).

4.5.4.2. Acute Systematic Toxicity

These studies indicated that the CSO and PS extracts of the HNS-Mo and control injected animals did not show any abnormality or significant loss in body weight during the

observation period and confirmed that the CSO and PS extracts of the HNS-Mo is non-toxic at the laboratory conditions simulated. Hence, the CSO and PS extracts of the HNS-Mo meet the requirements of the test as per the ISO 10993-11: 2017 (E), Annex A.7 & A.8: Test for systematic toxicity: Acute systematic toxicity test: Acute intraperitoneal & Acute intravenous application and USP 41/NF 36: 2018, systematic injection test.

4.5.4.3. Implantation of HNS-Mo

The main objective of this study was to evaluate the biological response of subcutaneous tissues to an implanted HNS-Mo after implantation. Macroscopically, there was no hemorrhage, encapsulation, discoloration, necrosis, or infection at the implant sites during any of the observation periods. Material debris was absent at the implant site both in the test and control group. The general physical conditions of the experimental animals were normal. None of the animals showed any abnormality or behavioral changes during the testing period. Tissue healing response was noted at the implant site in both groups after four weeks of implantation. The histopathological report indicated that the test material is non-irritant at one week and four weeks post-implantation. Hence the test material HNS-Mo meets the requirement of the test as per ISO: 10993-6: 2016 (E): Biological evaluation of medical devices: Part 6: Test for local effects after implantation: Annex A: Test method for implantation in subcutaneous tissues.

4.6. Discussion

The following are the main requirements of a new material developed for biomedical application:

(a) The application of the magnetic field should not influence it. (b) It should have sufficiently high strength with a good combination of toughness and ductility to ensure easy processing and stability of shape and design of devices manufactured with this material. (c) It should also have high corrosion resistance, fatigue strength and adequate

biocompatibility. The HNS-Mo stainless steel was studied in detail for all of its basic requirements to be used as a biomedical material.

4.6.1. Microstructure and Corrosion Resistance of HNS-Mo

The newly developed HNS-Mo was found austenitic, with negligible delta ferrite. The microstructure of stainless steels are highly dependent on their chemical constituents. The Schaffler diagram is helpful to estimate the microstructure based on the chemical components theoretically. To evaluate the microstructure using Schaffler diagram, nickel equivalent (Ni_{eq}) and chromium equivalent (Cr_{eq}) are used [51]. There should be a proper combination of these two elements to get an austenitic structure.

Theoretical values of Ni_{eq} and Cr_{eq} are estimated using **Eqs. 1.8 and 1.9** and presented in **Table 4.6**. It can be seen clearly that for the HNS and 316L, the relation $Ni_{eq} \geq Cr_{eq} - 8$ is satisfied. There is a deviation from this theoretical relation for the HNS-Mo; however, experimentally, it was found to have austenite microstructure with negligible ferrite, which was also present in the 316L. Manganese and molybdenum increase the solubility of nitrogen in austenitic stainless steel; however, molybdenum promotes ferrite formation [65]. The inclusions in the HNS-Mo were found according to the requirement of the ISO 5832-1 standard. Its grain size number was 6, which satisfies the ISO 5832-1 standard. The grain boundaries were found free of precipitates, which shows that the HNS-Mo will not be sensitised. It is one of the most important requirements of a material to be used for biomedical applications. The high amount of manganese increases the solubility limit of nitrogen in austenites and it was found in solution state. Also, the carbon in the HNS-Mo was limited to 0.034 wt%.

Table 4.6. Theoretical nickel equivalent, chromium equivalent, PREN and MARC values of the HNS-Mo, HNS and 316L austenitic stainless steels.

Material	Ni_{eq}	Cr_{eq}	PREN	PREN1	MARC
HNS-Mo	10.5	21.2	34.44	20.94	25.2
HNS	10.87	18.61	31.1	15.59	21.21
316L	11.36	19.42	23.5	21.70	20.28

Corrosion resistance of stainless steels depends on the chromium and molybdenum content. When nitrogen is added together with molybdenum, their synergistic effect significantly improves the corrosion resistance of stainless steel [64,182]. The theoretical pitting resistance of stainless steel in a chloride environment can be estimated by the pitting resistance equivalent number (PREN). The PREN number was calculated according to **Eq. 1.5** and is presented in **Table 4.6.** The HNS-Mo has the highest PREN value, whereas 316L has the lowest. In another study [82], the PREN formula was proposed for the manganese-containing stainless steels, as shown in **Eq. 1.6**. The PREN value (PREN1) was calculated accordingly and is presented in **Table 4.6**. PREN1 values are in agreement with the pitting potential obtained from potentiodynamic polarization tests. HNS has the lowest PREN1 and it has the lowest pitting potential **(Fig. 4.3)**. The HNS-Mo and 316L have comparable PREN1 and also have comparable pitting potential **(Table 4.2)**. Therefore, this equation (**Eq. 1.6**) is more suitable for the PREN values, to theoretically estimate the pitting resistance of manganese-containing stainless steels. The MARC values were also estimated using **Eq. 1.7** and are given in **Table 4.6**. MARC value is maximum for the HNS-Mo.

The HNS-Mo has the lowest corrosion rate when tested as per the ASTM G-48-11 method-A at a constant temperature of 22 °C for 24 hours, whereas 316L has the highest corrosion rate. The pitting potential of the HNS-Mo and 316L was comparable, whereas that of the HNS is the lowest. The better pitting resistance of the HNS-Mo as compared

to the HNS is due to the synergistic effect of molybdenum and nitrogen in the HNS-Mo. However, both the steels have comparable nitrogen. Lu et al. [64] showed the synergistic effect of Mo and N on pitting resistance. They suggested that nitrides form on the surface and protect the transpassive dissolution of molybdenum which causes retention of molybdenum in the passive surface and improves the localized corrosion resistance of stainless steel. Chao et al. [182] observed that the pitting resistance of the nitrogen-containing stainless steel increased significantly by the addition of molybdenum. The stainless steel having lower nitrogen content (0.39 wt%), when added with molybdenum (~ 2 wt%), showed a very high pitting potential as compared to the steel having higher nitrogen content (0.57 wt%) but zero molybdenum. Both the steels have comparable Cr and Mn content.

In this study, the critical current density of the HNS-Mo was found lower as compared to that of the 316L. Wan et al. [112] also found better corrosion resistance of nickel-free stainless steels containing molybdenum and nitrogen than the 317L, by electrochemical impedance spectroscopy (EIS). They found higher charge transfer resistance and impedance as well as lower capacitance for the nickel-free steels than the 317L. The charge transfer rate was found to decrease with an increase in nitrogen content, which signifies the role of nitrogen on the corrosion behavior of stainless steel. Li et al. [84] found higher pitting resistance for high nitrogen-containing steels than that of the 316L in 3.5 % NaCl solution. In the present study, the pitting potential of the HNS-Mo and 316L is similar. This disparity in results may be due to the difference in the molybdenum content. In previous studies [66,84,114], molybdenum content was more than 2 wt%, whereas in the present study, it is limited to 0.74 wt%.

4.6.2. Mechanical Behavior of HNS-Mo

The mechanical behavior of stainless steel depends mainly on the structure of matrix and alloy chemistry. The interstitial atoms in the solid solution have a significant influence on the strengthening of stainless steel. Nitrogen causes higher distortion in FCC lattice and it is more effective solid solution strengthening element than carbon [60]. Also, there is Cr-N short-range ordering in high nitrogen stainless steels [69,70]. Therefore, the HNS and HNS-Mo have higher strength as compared to that of the 316L. However, the HNS-Mo has higher strength than the HNS, which may be explained on the basis of the effect of its chemical components. Both the steels have similar nitrogen content and there is little difference in their chromium and manganese contents. However, Mo present in the HNS-Mo was found to form a short range order due to strong Mo-N bonding [183]. Short range ordering acts as obstacle to the dislocation motion and it causes increase in strength of the material.

The maximum stress corresponding to the endurance limit at 10^7 cycles of the HNS-Mo was found 513 MPa, in air, in which nitrogen content is 0.63 wt%. Park et al. [106] observed 475 MPa endurance limit for 0.59 wt% nitrogen content in Cr-Mn-N based stainless steel, similar to our HNS. There was much lower Mn content (10.39%) and Mo was absent. The yield strength and tensile strength were 537 and 928 MPa, respectively, whereas in the present case, it is 540 MPa and 933 MPa. Therefore, tensile strength is similar to that in the previous study, but there is a significant difference in endurance limits of these materials. The higher fatigue life and endurance limit of the HNS-Mo than HNS are due to the higher strength of the HNS-Mo [102]. It is suggested that material with higher yield strength causes less fatigue damage by decreasing the dislocation density [184]. Therefore, lower strength material induces a larger plastic zone and causes early initiation of slip band, promoting early crack initiation and fatigue failure. Thus,

higher number of cycles is observed for the HNS-Mo than HNS at the same stress condition. However, the endurance limit of the nitrogen steel is lower than the yield strength. The difference between yield strength and endurance limit (maximum stress) of the HNS-Mo (540-513) is 27 MPa, whereas it is 50 MPa for the HNS. This difference may be due to the presence of molybdenum in the HNS-Mo, which forms short-range ordering with nitrogen and may delay the process of crack initiation due to hindrance in dislocation movement.

The endurance limit (maximum stress) of the HNS-Mo was decreased from 513 MPa in air, to 475 MPa in SBF, which agrees with the earlier study [115,168]. The stress amplitude related to the maximum stress of 475 MPa, at a stress ratio of 0.1, will be ~ 213 MPa, which is higher than 200 MPa for the 316L [16]. Therefore, HNS-Mo has a higher endurance limit than the 316L in the SBF environment. The decrease in fatigue life, when tested in SBF, is due to the combined interaction of the SBF and cyclic loading. Passive film readily forms on the surface of stainless steel. However, due to cyclic loading, simultaneous destruction of the passive film occurs and the bare surface comes into contact of SBF. Thus, there is always a direct interaction of the material with corrosive media. Interestingly, the effect of SBF is prominent at lower stress levels, which may be due to the interaction of SBF with the material for a longer duration at lower stress than at higher stress. Thereby, SBF is more effective at lower stress.

4.6.3. Biocompatibility of HNS-Mo

The corrosion resistance and mechanical properties of the HNS-Mo were found comparatively better than those of the HNS and 316L. Further study was carried out on biocompatibility. Both *in vitro* and *in vivo* experiments were performed to evaluate the overall biological performance of the HNS-Mo. The L-929 mammalian and MG-63 human osteosarcoma bone cells adhered well on the surface and there was no inhibition

of the cell growth. HNS-Mo shows comparatively better cell response. It is to be mentioned that cell response is dependent on the ions released during the testing. The corrosion resistance of the HNS-Mo is comparatively better and also it has a negligible amount of nickel. Nickel-containing steel releases nickel in a higher quantity, which is toxic [185]. Cells contacting 316L are exposed to increased concentrations of nickel, a high amount of nickel impair BMP-2-induced ALP activity [56].

Additionally, *in vitro* cytotoxicity test for the HNS-Mo shows a numerical grade of 0 when tested with L-929 cells. The hematology results show blood compatibility. *In vivo* animal study indicated that this steel has no adverse effects and it is non-irritant and has no skin sensitization. Therefore, the Overall biocompatibility of the HNS-Mo is suitable according to the ISO standards.

4.7. Conclusions

A new grade of austenitic stainless steel with negligible amount of nickel (HNS-Mo) was designed and developed for biomedical applications, with the optimum composition of chromium, manganese, molybdenum and nitrogen. This steel is based on the CrMnMoN system. The HNS-Mo is designed with < 0.05% C, 19-20 % Cr, 19-20 % Mn, < 0.10% Ni, 0.50-1.0 % Mo, 0.60-0.70% N, < 0.50% Si, < 0.10% Cu and balance iron. Nickel was less than 0.10 wt%, as a trace element that is always present in the steel and derives from the raw materials, used for the melting. It was characterized for the microstructure, mechanical properties, corrosion, stress-controlled fatigue, corrosion fatigue and biocompatibility and was compared with these properties of the 316L and HNS. It has an austenitic microstructure, free from precipitation at the grain boundaries and is non-magnetic in nature. The HNS-Mo is superior in terms of mechanical properties like yield and tensile strength with adequate ductility. Thus, implants with lower thickness and weight can be manufactured with the HNS-Mo. Its corrosion resistance was found better

than those of the 316L and HNS. Its high cycle fatigue life and endurance limit corresponding to 10^7 cycles were higher than that of HNS and 316L. The *in vitro* biocompatibility study shows that the HNS-Mo did not inhibit the cell growth and attachment and was better than that of the 316L. The *in vivo* biocompatibility study confirmed the usefulness of this material and did not cause any inflammation and toxic effect. It was found non-irritant and biocompatible. The cost of this material will be lower by ~ Rs 100 per kg as compared to the 316L, as it does not contain costly nickel. Therefore, the HNS-Mo combines the benefits of strength with adequate ductility, stable austenite structure, better corrosion resistance and fatigue strength with acceptable biocompatibility. Overall, this HNS-Mo austenitic stainless steel with negligible nickel is found to be a potent replacement of 316L. Furthermore, to be used as an implant material, it needs approval for clinical trials.